ISSN 1330-3651 (Print), ISSN 1848-6339 (Online)
https://doi.org/10.17559/TV-20230327000482
Original scientific paper

The Time Response Analysis of a Hybrid Electronic Switch and Residual Current Devices System

Ahmet YURTCU, Mustafa YAGIMLI*, Hakan TOZAN

Abstract: Residual current devices are vital as they are used to protect humans from electric shocks and fire hazards. These devices detect the residual current in the grid, open the mechanism, and leave the grid without voltage. In this study, the time response of a newly designed hybrid system consisting of an electronic switch system and a residual current device to protect humans from hazards has been analyzed. A model consisting of capacitors and resistors has been used to simulate the human body. In the designed system, the average response time was found to be 1.37 ms, which operates with an average of 6.43 times faster than a conventional residual current device. The results of the study illustrated that the designed system leaves the circuit voltage-free much faster than a conventional residual current device and is more effective in protecting human life.

Keywords: circuit implementation; electronic switch; residual current device; time response analysis

1 INTRODUCTION

The conventional residual current devices (RCD) which are vital for human life protection continuously compare the current in phase with the current in a neutral phase [1]. In conventional RCD, when the gap reaches 30 mA (the freezing current threshold), the relay activates, pushes the contact near it, opens the circuit, and leaves it without voltage. Fuses and circuit breakers are not capable of performing this task of RCDs [3].

There are many studies conducted on conventional RCDs. Mitolo in 2010 evaluated the success of the use of RCDs [4]. Shopov et al. presented a study on the analysis of the behavior of the different models of RCDs working with frequencies over 50 Hz (resp. 60 Hz) [5-6]. Xie et al. presented the tripping characteristics of RCDs under different working conditions, and the minimum tripping currents of the RCD samples were recorded [7]. Freschi analyzed the behavior of RCDs at frequencies higher than the rated frequency and developed a mathematical model [8]. Czaja analyzed RCDs with different designed release systems and illustrated their effects on release frequency range [9]. Utegulov et al. have developed a method to increase the efficiency of RCDs below 1000 volts based on direct installation [10]. Porta et al. performed a study on faulty switches of RCDs in circuits feeding electronic loads [11]. In testing the ground loop impedance or resistance at low voltage power, systems become inconvenient when RCDs are loaded. Therefore, it is not practical to test unwanted switches with conventional methods [12]. Czapp et al. proposed a new method to test the effectiveness of automatic feed interruption without unwanted switches [13]. Salvatierra et al conducted a study at 127 volt which was the medium voltage in housing and industry in Ecuador, where electrical accidents were very common [14]. Espinoza et al. measured the time response analysis of a conventional residual current relay, and the laboratory results showed that a conventional protection relay could be opened in an average of 8.81 milliseconds [15]. Kolarik presented the operation principle of admittance protection, calculation, and recommendation for activating admittance protection for 20 kV feeders in a system with low-ohmic and parallel compensation grounding [16]. Alidemaj et al. analyzed the performance of the circuit breaker during the disconnection of the failure currents due to the asynchronous connection of the generator on the grid and emphasized the importance of studying the network for each specific case for dimensioning of generator breakers [17]. Nikolovski et al. presented a procedure and computation of relay protection coordination for a photovoltaic power plant connected to the distribution network [18]. Heidary et al. focused on the analysis of transient recovery voltage (TRV) under the presence of an inductive-based superconducting fault current limiter installed in a power grid, and then it investigated the impact of a controllable superconducting series reactor in TRV of the circuit breaker [19].

In this study, the time response of a hybrid system which consists of an electronic switch and a residual current device, has been analyzed using a human body model (HBM) formed using capacitors and resistors [15, 20-21].

1.1 The Designed System

The block diagram of the designed system is shown in Fig. 1. The designed system consists of two separate blocks. The first block is the power circuit which controls the transmission of power to the system. The second block, the logic circuit, provides control of the power circuit. A PIC series microcontroller is used to control the logic circuit. In the power circuit, a toroidal transformer was used to ensure the operation of the residual current device. In addition, triacs were triggered at the zero crossing point of the alternative signal using a MOC series optocoupler.

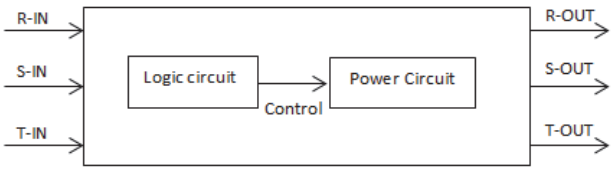

Figure 1 Block diagram of the designed system

The circuit diagram of the power stage is shown in Fig. 2. 3 Phase inputs (R-IN / S-IN / T-IN) are transferred to the output (R-OUT / S-OUT / T-OUT) with T1/T2-T3 triacs

passing through the toroidal transformer named trigger coil shown on the logic card. Triacs belonging to each phase are driven by MOC3041M (OK-1/OK-2/OK3), which is an optodiac integrated circuit containing a zero cross detector. It is optically isolated from the logic circuit.

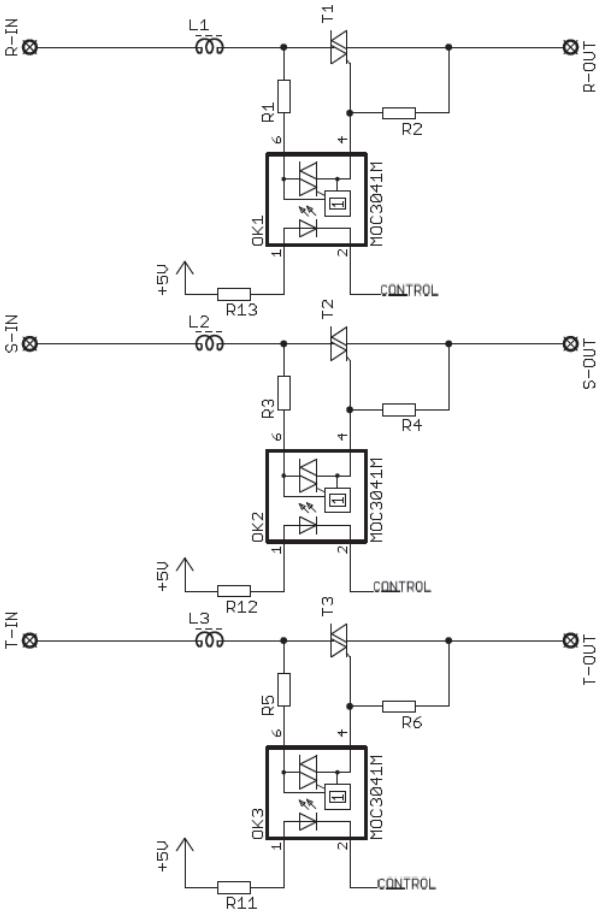

Figure 2 Power circuit diagram

The circuit diagram of the logic stage is shown in Fig. 3. Three pins of PIC 12C508 microcontroller are used in the circuit. With a push button connected to the GP2 pin, the system can be activated or deactivated. On this toroidal transformer, where *L*1 - *L*2 - *L*3 coils on the GP1 pin power stage are wound, 1200 turns of trigger coil with 0.2 mm cross-section were located. Thus current flow to the ground rather than the load current flowing through the *L*1 - *L*2 - *L*3 coils, is felt sensed. Since this voltage induced at the time of the error is AC, it is rectified with the *B*1 bridge diode and applied to the GP1 pin. 4.7 Volt zener diode (*D*1) is used to protect the microcontroller from overvoltage. The GP0 pin is the control output of the microcontroller. The NPN is buffered by a transistor as three MOC3041 will be triggered at the same time. The positive trigger signal applied to this transistor enables the optodiacs of each phase in the power stage to complete the circuit with the GND pins. However, the MOC3041 integrated circuit does not start at this moment and waits for the zero points of each phase. This period takes up to 1/100 second. This is because there are 100 alternans in total in the AC signal with a frequency of 50 Hz [2].

HBM is shown in Fig. 4. This model is a study to provide a theoretical model of currents flowing in lightning strike injuries.

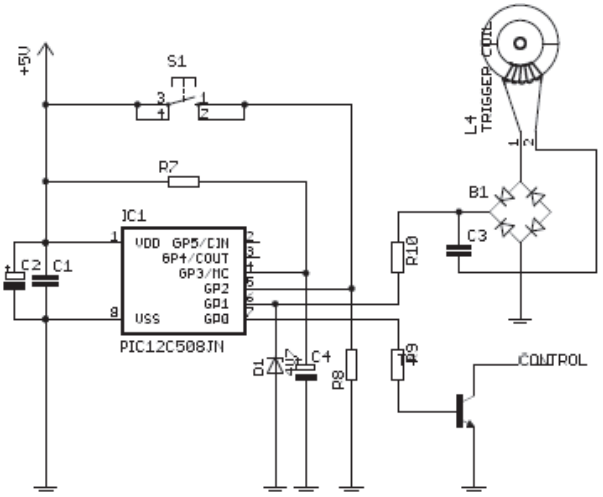

Figure 3 Logic circuit diagram

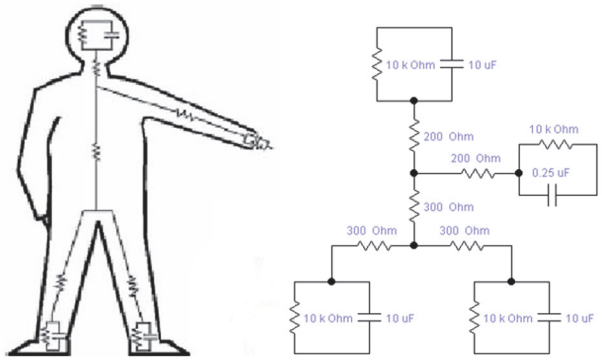

Figure 4 Human body model [19]

As an internal component, the arms contain only an internal resistance between the torso and the legs. Surface resistance components are significantly greater than internal resistance. It consists of 10 kΩ parallel resistance and 0.25 μF capacitance. This body model is required to model external and skin distortions when activated by a lightning current source. Although this HBM was developed for high current effects, it can be used at low current levels [22].

1.2 Time Response Analysis

For measurements, RIGOL DS1102E digital oscilloscope is used where the limbs of the human body, that can be exposed to current, are modeled as the right arm, left arm, right foot left foot, and head. The residual current that may occur in those limbs is measured according to the resistance values of Espinosa et al. [15] as 560 Ω, 1 kΩ, and 10 kΩ with the same HBM.

2 RESULTS

This study has been analyzed in HBM with low voltage against electric shock at residential and industrial levels.

A load of 560 Ω was used in the four cases presented below. Similar to Espinosa et al. [15] 200 samples were analyzed.

In the first case, 127 V source input is connected on the left arm, and the right and left legs are in contact with the ground. Points in contact with the ground are kept at ground level. Fig. 5 shows the time response when the left

arm is exposed to the current. In Fig. 5, there is a signal flow between −0.4 and 0.6 ms, and the current was obtained as zero in other time intervals.

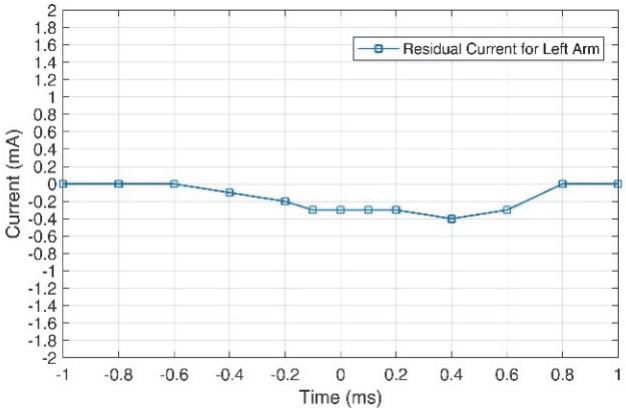

Figure 5 Current signal corresponding to the developed system activated for contact with the left arm

In the second case, there is a 127 volt source input on the right arm and the left and right legs have been in contact with the ground. Fig. 6 shows the analysis that occurs when the right arm is exposed to current at a load of 560 Ω.

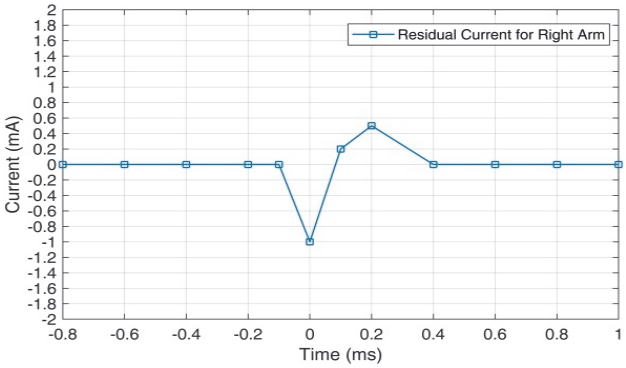

Figure 6 Current signal corresponding to the developed system activated for contact with the right arm

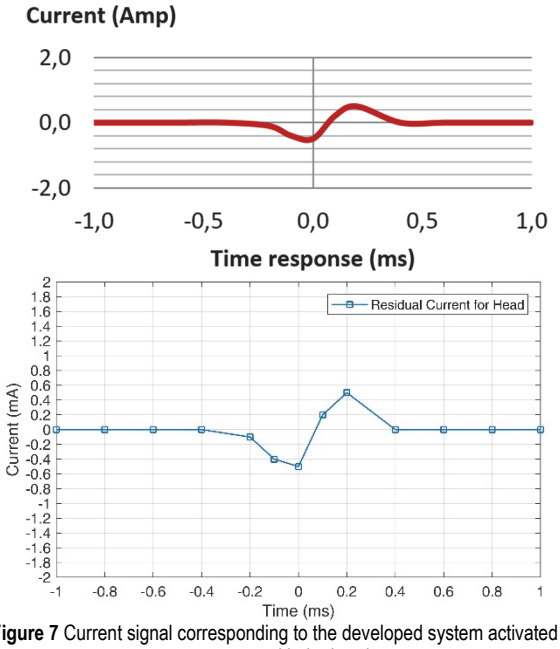

Figure 7 Current signal corresponding to the developed system activated for contact with the head

In the third case, there is a 127 volt source input directly on the head, and the left and right legs are in contact with the ground. Fig. 7 shows the results of the analysis performed in case the head is exposed to current.

In the fourth case, the 127 volt source was connected to the left leg while the right arm was kept at ground level. Fig. 8 shows the time response if the left foot is exposed to the current.

Finally, the 127 volt source was attached to the right leg while the left arm was kept at ground level. Fig. 9 simulates the analysis that occurs when the left foot is exposed to a current.

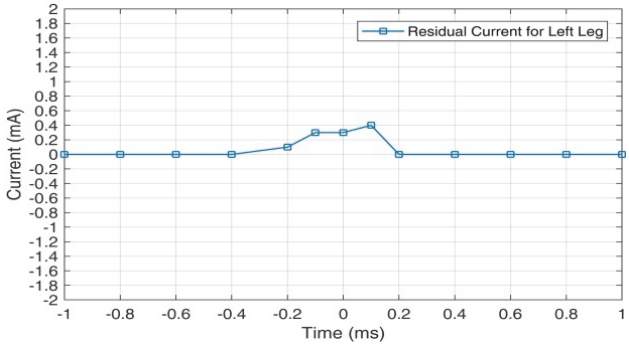

Figure 8 Current signal corresponding to the developed system activated for contact with the left leg

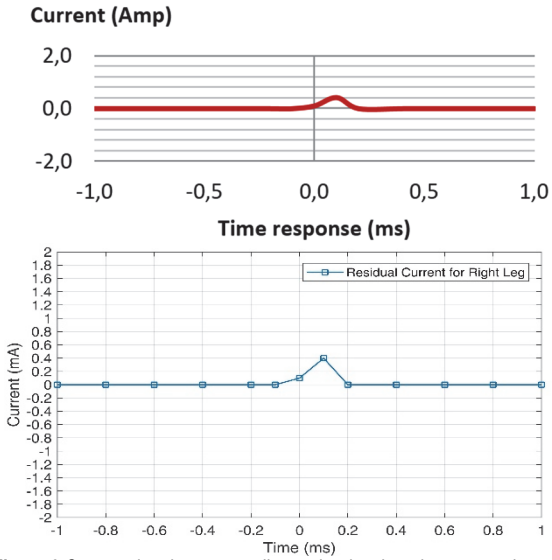

Figure 9 Current signal corresponding to the developed system activated for contact with the right leg

Similar tests have been done by changing the load resistance to 1 kΩ and 10 kΩ. The summary of these test results is presented in Tab. 1. In addition, all measurements made in Tab. 1 have different load resistances for each part of the body. Six measurements are presented in Tab. 1.

Tab. 2 shows a summary of the time response results of 200 measurements, taking into account the minimum and maximum time response for each body part. The average duration was also calculated.

Fig. 10 shows the data of Tab. 1. On the other hand, from the measurements taken from 200 samples, the average of six people can be seen. Data at a point shows individual data.

Table 1 System response times

Load resistor	Parts	t_1 / ms	t_2 / ms	t_3 / ms	t_4 / ms	t_5 / ms	t_6 / ms
	Left arm	1,25	1,24	1,26	1,28	1,30	1,30
	Right arm	1,24	1,23	1,24	1,27	1,29	1,29
560 Ω	Head	1,26	1,27	1,27	1,29	1,32	1,31
	Left leg	1,28	1,29	1,30	1,31	1,33	1,32
	Right leg	1,29	1,30	1,32	1,32	1,34	1,34
	Left arm	1,26	1,30	1,32	1,32	1,33	1,33
	Right arm	1,26	1,32	1,34	1,34	1,35	1,36
1 kΩ	Head	1,25	1,26	1,28	1,30	1,34	1,36
	Left leg	1,27	1,31	1,33	1,35	1,36	1,38
	Right leg	1,28	1,29	1,32	1,34	1,35	1,38
	Left arm	1,24	1,28	1,31	1,35	1,38	1,40
	Right arm	1,25	1,26	1,32	1,36	1,37	1,39
10 kΩ	Head	1,26	1,28	1,32	1,38	1,41	1,45
	Left leg	1,27	1,29	1,35	1,40	1,42	1,44
	Right leg	1,27	1,29	1,33	1,42	1,47	1,50

Table 2 Analysis of minimum, maximum and average time

Load resistor	Parts	Minimum time / ms	Average time / ms	Maximum time / ms
	Left arm	1,25	1,28	1,30
	Right arm	1,23	1,26	1,29
560 Ω	Head	1,26	1,29	1,32
	Left leg	1,28	1,31	1,33
	Right leg	1,29	1,32	1,34
	Left arm	1,26	1,30	1,33
	Right arm	1,26	1,31	1,36
1 kΩ	Head	1,25	1,31	1,36
	Left leg	1,27	1,33	1,38
	Right leg	1,28	1,33	1,38
	Left arm	1,24	1,32	1,40
	Right arm	1,25	1,32	1,39
10 kΩ	Head	1,26	1,36	1,45
	Left leg	1,27	1,36	1,44
	Right leg	1,27	1,39	1,50
Total	Averages	1,26	1,32	1,37

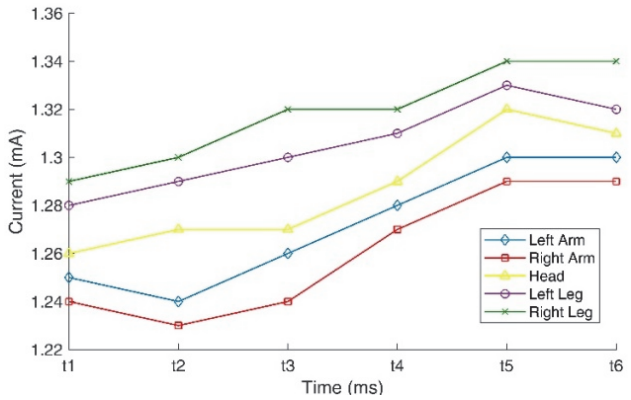

Figure 10 Graph of the trend of time in milliseconds at every part of the body with 560 Ω load

3 CONCLUSION

In his study, the time response (cut-off times) of a hybrid system which consists of an electronic switch and a residual current device to protect humans from hazards, has been analyzed under different scenarios. As can be seen in Tab. 2, the average of the maximum time in the developed system was measured as 1.37 ms. This value is 8.81 ms in the works of Espinazo et al. performed with the traditional residual current relay. Results of the measurement showed that the developed system operates 6.43 times faster than the conventional residual current devices in means of time.

The reason for closer response times is that the activation time and the exposed organ stand still in measurements. Thus no matter which organ is exposed the reaction time does not change as the system energy is switched off.

4 REFERENCES

[1] Czapp, S. (2007). Protection Against Electric Shock Using Residual Current Devices in Circuits with Electronic Equipment. *ElectronikaIrElektrotechnika, 76*(4), 51-54.

[2] Yagimli, M. & Tozan, H. (2020). *Occupational Health and Safety in Electric Works*. Sixth edition, Beta Publisher, 76, ISBN:978-605-242-735-4.

[3] Atkinson, B., Lovegrove, R., & Gundry, G. (2013). *Electrical Installation Design*. Fourth Edition, 213. https://doi.org/10.1002/9781118477786

[4] Mitolo, M. (2010). Shock Hazard in the Presence of Protective Residual-Current Devices. *IEEE Transactions on Industry Applications*. 46(4). 1552-1557. https://doi.org/10.1109/TIA.2010.2051068

[5] Shopov, Y., Filipova-Petrakieva, S., & Boychev, B. (2018). Investigation of Residual Current Devices in High Frequencies. *10th Electrical Engineering Faculty Conference (BulEF)*, 1-3. https://doi.org/10.1109/BULEF.2018.8646945

[6] Slangen, T. M. H., Lustenhouwer, B. R. F., Ćuk, V. & Cobben, J. F. G. (2021). The Effects of High-Frequency Residual Currents on the Operation of Residual Current Devices. *19th International Conference on Renewable Energies and Power Quality*, *19*, 67-72. https://doi.org/10.24084/repqj19.216

[7] Xie, P., Fang, Z., Hu, J., Yang, J., & Zhu, G. (2019). Tripping Characteristics of Residual Current Devices Under Different Working Conditions. *2019 IEEE 3rd Conference on Energy Internet and Energy System Integration (EI2)*, 2765-2769. https://doi.org/10.1109/EI247390.2019.9062090

[8] Freschi, F. (2012). High-Frequency Behavior of Residual Current Devices. *IEEE Transactions on Power Delivery*, 27(3). 1629-1635. https://doi.org/10.1109/TPWRD.2012.2191423

[9] Czaja, P. (2017). Examination of the impact of design of a Residual Current Protective Device on the release frequency range. *Progress in Applied Electrical Engineering (PAEE)*, 1-5. https://doi.org/10.1109/PAEE.2017.8009009

[10] Utegulov, B. B.,Utegulov, A. B., & Uakhitova, A. B. (2016). Development of Method to Improve Efficiency of Residual Current Device under 1000 V on Excavators of Mining Enterprises. *Journal of Mining Science*, *52*(2), 325-331. https://doi.org/10.1134/S1062739116020477

[11] Roldan-Porta, C., Escriva-Escriva, G., Carcel-Carrasco, F. J., & Roldán-Blay, C. (2014). Nuisance tripping of residual current circuit breakers: a practical case. *Electr. Power Syst. Res.* 106. 180-187. https://doi.org/10.1016/j.epsr.2013.07.020

[12] Stanislaw, C. & Borowski, K. (2019). Verification of safety in low-voltage power systems without nuisance tripping of residual current devices. *Electric Power Systems Research*, *172*, 260-268. https://doi.org/10.1016/j.epsr.2019.03.027

[13] Czapp, S., Borowski, K., Dobrzynski, K., Klucznik, J. &Lubosny, Z. (2015). A new method of fault loop resistance

measurement in low voltage systems with residual current devices. *IEEE Eindhoven PowerTech*, 1-5. https://doi.org/10.1109/PTC.2015.7232279

[14] Salvatierra, B. G., Dominguez, D. H., & Morales, J. A. (2015). Analysis of electric shock human safety to residential, industrial and medium voltage levels. *IEEE International Autumn Meeting on Power, Electronics and Computing (ROPEC)*, 1-6. https://doi.org/10.1109/ROPEC.2015.7395085

[15] Espinoza, C., Villavicencio, F., Cuzco, O., & Aguilar, J. (2017). Time Response Laboratory Analysis for Residual Current Devices. *IEEE PES Innovative Smart Grid Technologies Conference*, 1-6. https://doi.org/10.1109/ISGT-LA.2017.8126726

[16] Kolarik, M. (2020). The Application of Admittance Relay Protection for Earth Fault Detection in Distribution Medium Voltage Grid. *Polytechnic and design*, *8*(1), 1-7.

[17] Alidemaj, A., Škuletić, S., & Radulović, V. (2017). Fault current due to asynchronous connection of the generator to the grid and impact on HV circuit breaker with gas SF6. *Tehnički vjesnik*, *24*(6), 1813-1819. https://doi.org/10.17559/TV-20160128145656

[18] Nikolovski, S., Papuga, V., & Knežević, G. (2014). Relay Protection Coordination for Photovoltaic Power Plant Connected on Distribution Network. *International journal of electrical and computer engineering systems*, *5*(1), 15-20.

[19] Heidary, A., Cheshmeh Beigi, H. M., & Mehrizi-Sani, A. (2021). Impact of controllable superconducting series reactor in transient recovery voltage of circuit breaker. *Transformers Magazine, 8*(S5).

[20] Yagimli, M. & Yurtcu, A. (2020). Development of a Hybrid System with Electronic Switch and Residual Current Relay, *International Journal of Advances in Engineering and Pure Sciences,* 32(4), 467-472. https://doi.org/10.7240/jeps.703025

[21] Yurtcu, A., Yagimli M., & Tozan, H. (2020). A Low-Cost Hybrid System of a Zero-Crossing Switch and Leakage Current Relay. *ICAT'20 International Conference on Advanced Technologies*.

[22] Andrews, C. (2003). *Electrical aspects of lightning strike to humans*, Fifth edition, The Lightning Flash, IEEE Press, London, 548-564. https://doi.org/10.1049/PBPO034E_ch11

Contact information:

Ahmet YURCU, PhD
Occupational Health and Safety Program, Merzifon Vocational School,
Amasya University, 05300, Amasya/Turkey
E-mail: ahmet.yurtcu@amasya.edu.tr

Mustafa YAGIMLI, PhD
(Corresponding author)
Department of Computer Engineering, Istanbul Gedik University,
Yakacık, 34876, Istanbul/Turkey
E-mail: mustafa.yagimli@gedik.edu.tr

Hakan TOZAN, PhD
College of Engineering and Technology,
American University of the Middle East, Egaila 54200, Kuwait
E-mail: hakan.tozan@aum.edu.kw